## **Supporting Information for:**

## A Rapid and Label-Free Strategy to Isolate

## Aptamers for Metal Ions

 $Hao\ Qu^{\dagger},\ Andrew\ T.\ Csordas^{\sharp},\ Jinpeng\ Wang^{\dagger},\ Seung\ Soo\ Oh^{\S},\ Michael\ S.\ Eisenstein^{\sharp},\ Hyongsok$   $Tom\ Soh^{\#*}$ 

\*Corresponding author.

# Current address: Department of Electrical Engineering and Department of Radiology, Stanford University, Stanford, CA 94305 (USA)

This Supporting Information section contains the following materials:

Table S1, Experimental conditions for SS-PD screening of Hg<sup>2+</sup> and Cu<sup>2+</sup>

Table S2, Hg<sup>2+</sup> and Cu<sup>2+</sup> selected aptamer sequences

Figure S1, Hg<sup>2+</sup> folding screen data

Figure S2,  $Hg^{2+}$  R4 pool binding measurements

Figure S3,  $K_D$  measurement results for  $Hg^{2+}$  aptamers

Figure S4, Cu<sup>2+</sup> folding screen data

Figure S5, Cu<sup>2+</sup> R3 pool binding measurements

**Table S1:** Experimental conditions for SS-PD screening of  $Hg^{2^+}$  and  $Cu^{2^+}$ .  $Hg^{2^+}$ 

 $Cu^{2+}$ [T] 400 μΜ 1 mM # of AP sorted  $1 \times 10^{8}$  $1 \times 10^{8}$ Round 1  $3.4 \times 10^{5}$  $3.8 \times 10^{5}$ # of AP collected 100 μΜ [T]  $1 \, \text{mM}$  $1 \times 10^7$  $1 \times 10^7$ Round 2 # of AP sorted # of AP collected  $5.0 \times 10^{4}$  $3.8 \times 10^{5}$ [T] 500 μΜ 25 μΜ # of AP sorted  $1 \times 10^7$  $1 \times 10^7$ Round 3  $4.0 \times 10^{4}$  $2.3 \times 10^{4}$ # of AP collected 50 μΜ N/A [T]  $1 \times 10^7$ N/A # of AP sorted Round 4  $8.4 \times 10^{4}$ # of AP collected N/A

**Table S2:** Hg<sup>2+</sup> and Cu<sup>2+</sup> selected aptamer sequences.

Hg <sup>2+</sup> aptamer sequences selected region (5' to 3')	$IC_{50} (\mu M)$
GGAAAAAGGA TTT CTGCXXCGATTCTTG TTT TTTGCGCATAGCCCAACCGG	$12.72 \pm 5.26$
GAGCGTGTTA TTT CTGXXTGCGATTCTTG TTT CAAACTCCATCCTACATACG	$26.35 \pm 6.21$
ACCCGAGATA TTT CTGTAGCAATTCTTG TTT AGAGCTAAGTTTTTACGAGC	$14.40 \pm 5.00$
GCCACGCTGT TTT CTGCGGCGATCCTTG TTT GTCCTCAAAATTCATTAGGG	$10.49 \pm 8.43$
TCAAAAAGTC TTT CTGCAACGATCTTTG TTT AGGGTGATCTAGTCTACCAC	$14.16 \pm 4.75$
TGATAAACCG TCT CTGCAGCCATTCTTG TTT CGCAGCAAGCTGAAAAGGTC	23.11 ± 12.46
TCCAAGCTCT TTT CTGCAGCTATTCTTG TTT CGAAACTTGCTAAGCTGCGT	$2.27 \pm 0.76$
(SSA-HgII)	
Cu <sup>2+</sup> aptamer sequences selected region (5' to 3')	$IC_{50} (\mu M)$
GTCATTAAAC TXX XXXCAGCGATTCTTG TTT ATAGGCCCGGGTTCCTGATA	$72.94 \pm 30.64$
ATCGCGATAT TTT CTGTAGCGATTCTTG TTT GAGCGCTCGGTACGAACAGA	47.15 ± 22.16
(SSA-CuII)	

Primer-binding sequences are omitted; mutated sites are shown in red, and deleted bases are shown with a red "X". The sequence of the starting library is as follows: 5'-cctctctatgggcagtcggtgat-[10N]-TTT-CTGCAGCGATTCTTG-TTT-[20N]-ggagaatgaggaacccagtgcag-3', where lowercase letters indicate primer-binding regions.

## Hg<sup>2+</sup> folding screen data

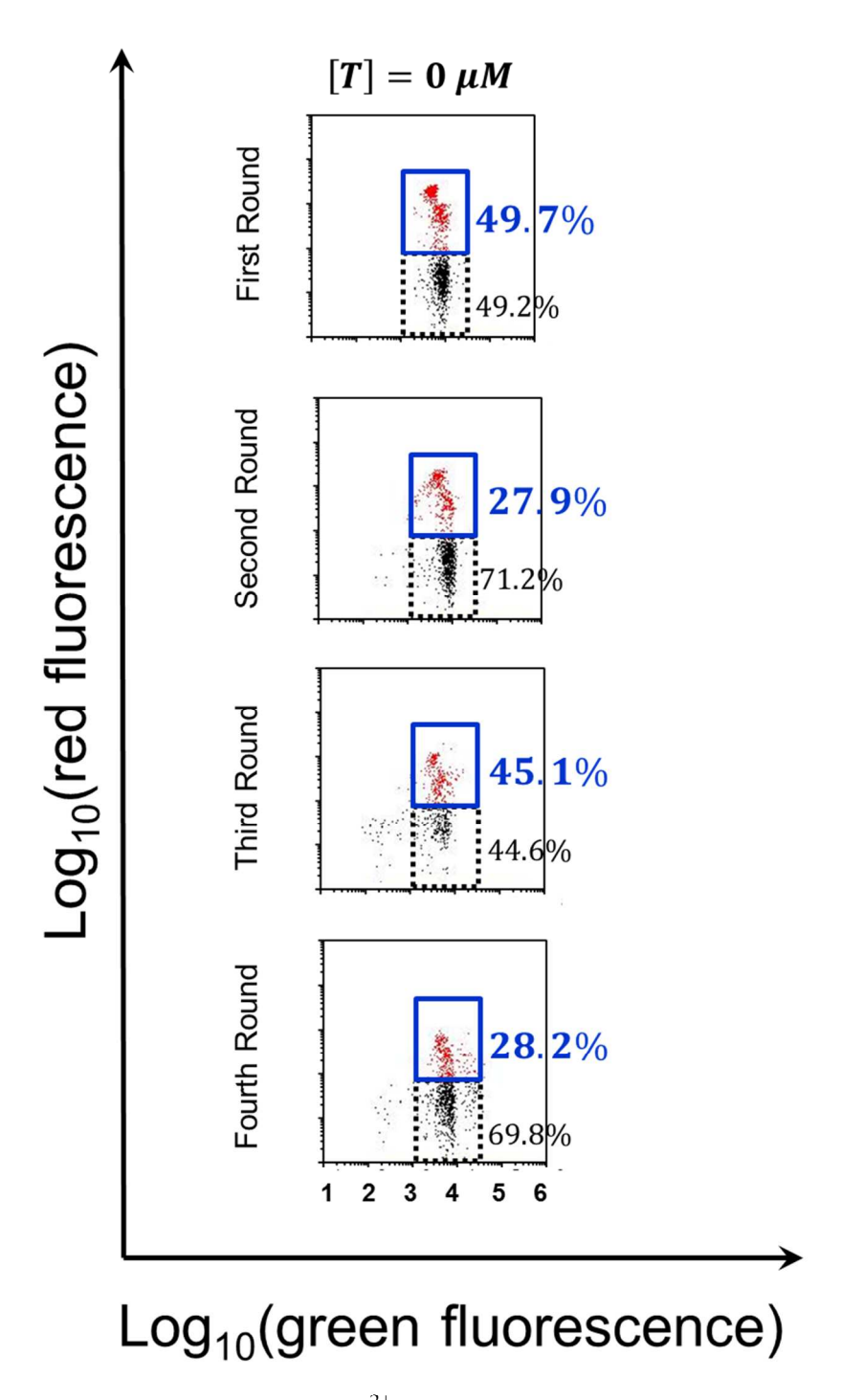


**Figure S1**. Folding screen results for Hg<sup>2+</sup>. Solid blue boxes indicate the sorting gate for aptamers that retained both red and green reporters in the absence of target. The black dashed boxes show sequences that are unable to hybridize to the red reporter; these sequences are

discarded and not carried on the next round. This step removes aptamers from the population that undergo self-hybridization without target present. We believe the main reason for the persistence of these "false-positive" sequences is due the strong selection pressure during the "binding screen" which favors sequences capable of "kicking-off" the red-porter, allowing them to remain in the pool. In addition, errors during PCR may introduce sequences with mutations in the constant region which will prevent binding of the red reporter, allowing a sequence to appear as a false positive. Nevertheless, we were able to eliminate the majority of these false-positives and obtain true structure switching aptamers for both Hg<sup>2+</sup> and the Cu<sup>2+</sup>.

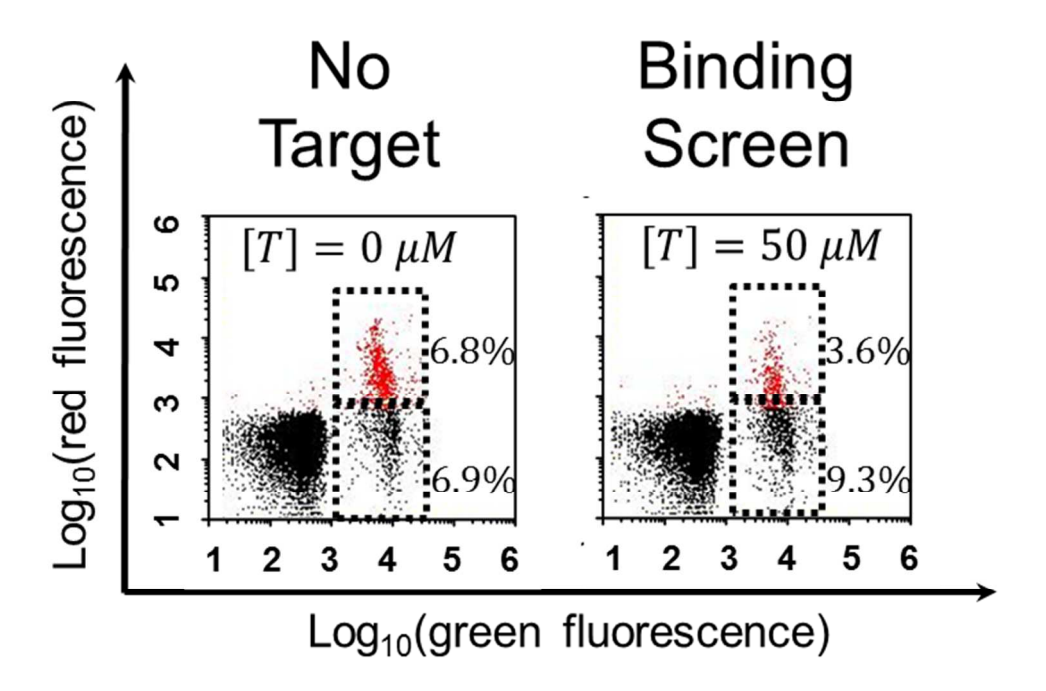


**Figure S2**: Binding measurements for the final  $HgCl_2$  R4 pool. R4 pool aptamers exhibited minimal additional shift in red fluorescence relative to the previous R3 pool (see Fig 3A, row 4) when challenged with 50  $\mu$ M  $Hg^{2+}$ .

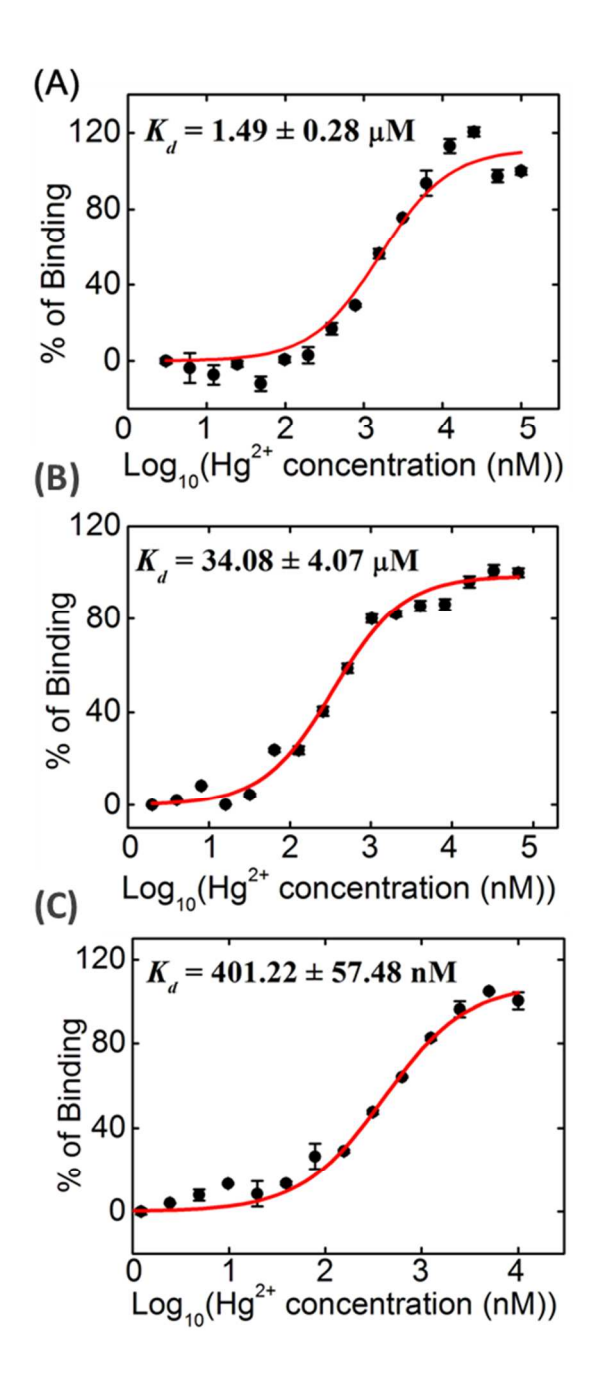


**Figure S3**.  $K_D$  measurements from microscale thermophoresis assays for (A) SSA-HgII, (B) HgA, a previously reported Hg<sup>2+</sup> aptamer (5'-TTCTTTCTTCCCCTTGTTTGTT-3')<sup>29</sup>, and (C) truncated SSA-HgII with the central constant domain removed). Error bars represent the standard deviation of two measurement trials, and the red solid lines are the fit using  $\eta=1/(1+K_D/[\text{Ligand}])$ , where  $\eta$  is the binding fraction. Each  $K_D$  obtained from microscale thermophoretic measurements shows an excellent fit to the Langmuir isotherm.

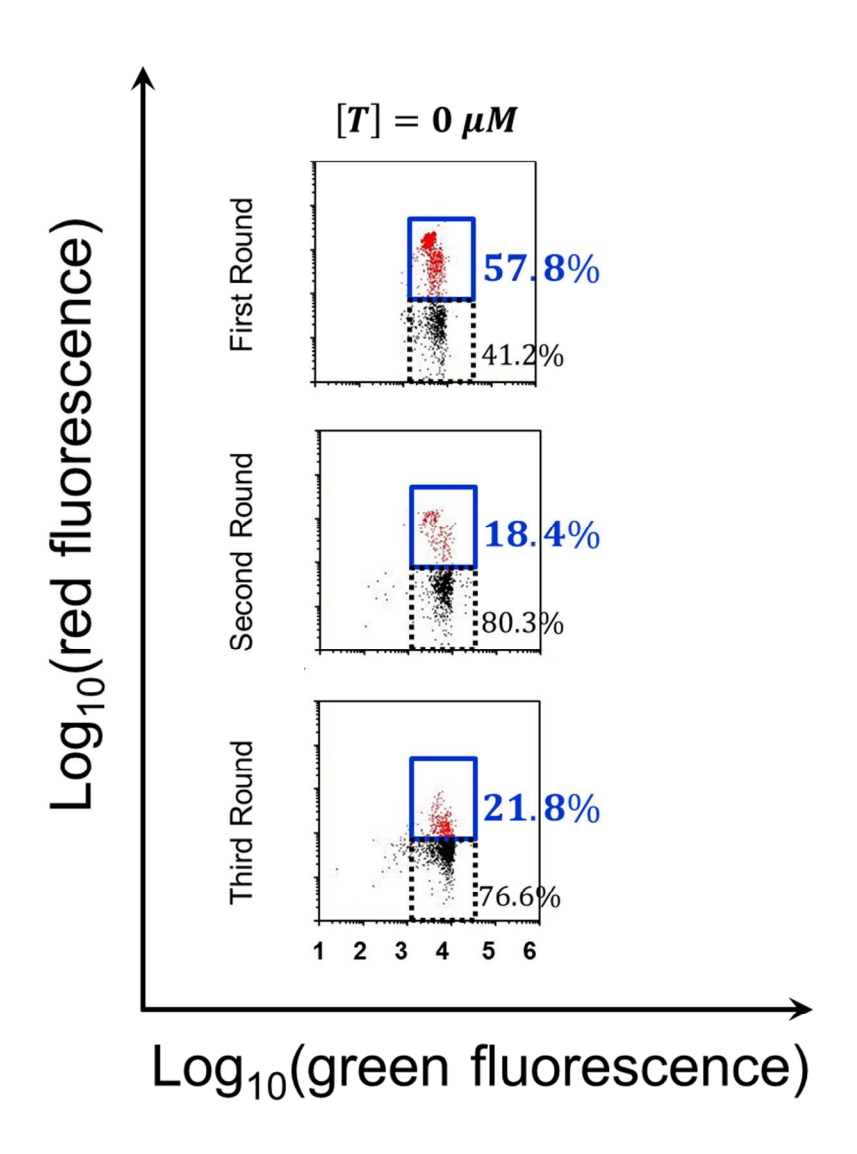


**Figure S4**. Folding screen results for Cu<sup>2+</sup>. Data are presented in the same format as for Figure S1.

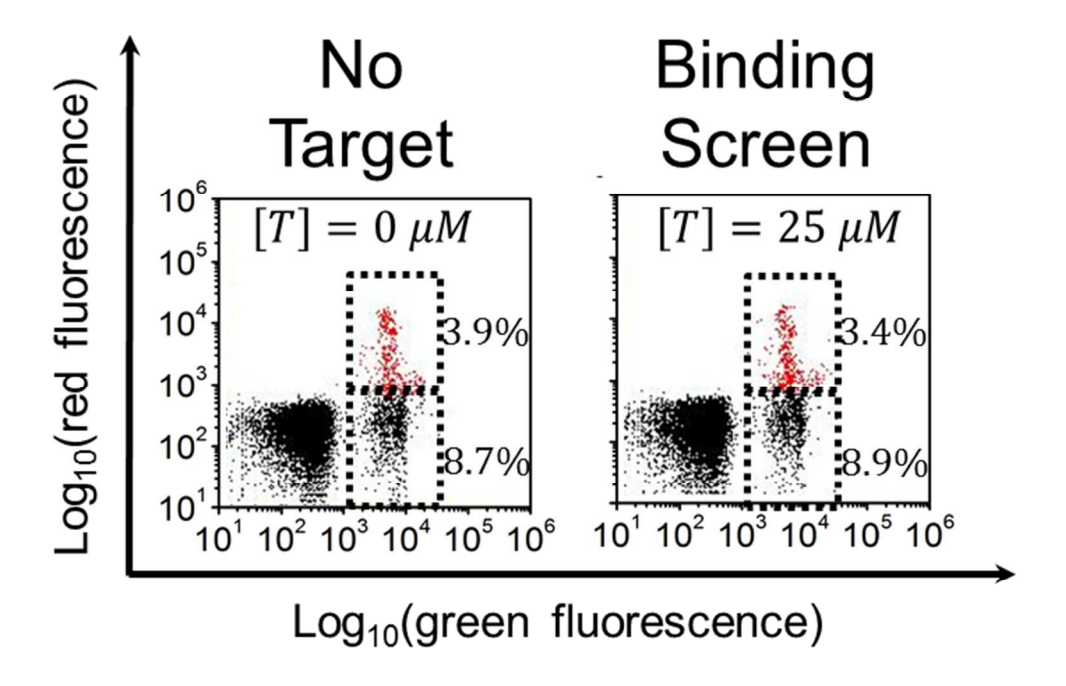


**Figure S5**: Binding measurements for the final  $CuCl_2$  R3 pool. R3 pool aptamers exhibited minimal additional shift in red fluorescence relative to the previous R2 pool (see Fig 4A, row 3) when challenged with 25  $\mu$ M  $Cu^{2+}$ .